A Weak-wind Zone Accompanied with Swelled Snow Clouds in the Upstream of a Low-altitude Ridge —Single Doppler Radar Observations over the Tsugaru District of Japan—

By Yasu-Masa Kodama

Department of Earth and Environmental Sciences, Hirosaki University, Hirosaki, Japan

Masayuki Maki[1]

National Research Institute for Earth Science and Disaster Prevention, Tsukuba, Japan

Shin-ichi Ando,[2] **Masaya Otsuki,**[2] **Osamu Inaba,**[3] **Jun Inoue,**[4] **Naoya Koshimae**[5]

Department of Earth Sciences, Hirosaki University, Hirosaki, Japan

Sento Nakai and Tsuruhei Yagi

National Research Institute for Earth Science and Disaster Prevention, Tsukuba, Japan

(Manuscript received 15 August 1997, in revised form 8 July 1999)

Abstract

When the winter monsoon prevails over the Japan Sea, many shallow convective snow clouds appear in the atmospheric mixed layer, and provide much snow over Japan. The behavior of the snow clouds and airflow affected by a complex terrain in the Tsugaru district of Japan, was studied based on single Doppler-radar observations. At $\sim$ 15 km upstream of the Tsugaru mountains, which is a low-altitude (200–700 m ASL) ridge, a weak-wind zone accompanied by upward developing snow clouds appeared parallel to the mountains. Above and in the lee of the Tsugaru mountains, the tops of the snow clouds were significantly lower towards the east accompanied with wind acceleration. In accordance with a theory of 2–D two-layer flow passing over a ridge, sonde-observed environmental parameters described a flow regime, where the flow is partially blocked and associated with a hydraulic lee jump. The observed flow pattern was consistent to this theoretical prediction, although the hydraulic lee jump could not be conclusively identified due to observational difficulties. Low-level wind convergence in the front of the weak-wind zone sustained the upward development of the snow clouds. The upward development of the snow clouds, however, did not lead to an obvious increase of snowfall intensity. A WSW to ENE elongated zone of increased snowfall appeared from the north of the Shirakami mountains and Mt. Iwaki (both high-altitude mountains with peaks exceeding 1000 m ASL), to Mutsu Bay, passing through a corridor of the Tsugaru mountains. The orographic effects of the Shirakami mountains, Mt. Iwaki, and the corridor of the Tsugaru mountains were examined with respect to maintaining this elongated snowfall zone.

Corresponding author: Yasu-Masa Kodama, Department of Atmospheric and Environmental Sciences, Hirosaki University, 3 Bunkyo-cho, Hirosaki, Aomori 036-8561, Japan. E-mail: kodama@cc.hirosaki-u.ac.jp

1 Present affiliation: Meso scale Meteorology Group, Bureau of Meteorology Research Centre, Melbourne, VIC 3127, Australia

2 Present affiliation: Hokkaido Headquarters, Japan Weather Association, Sapporo 064-0824, Japan

3 Present affiliation: Sendai District Meteorological Observatory. Japan Meteorological Agency, Sendai 983-0842, Japan

4 Present affiliation: Institute of Low Temperature Science, Hokkaido University, Sapporo 060-0819, Japan

5 Present affiliation: HOKKAIDO CHIZU Co., Ltd., Asahikawa 070-8022, Japan

1. Introduction

When a cold continental airmass developed over the Siberia plains flows out as a winter monsoon over the Japan Sea of relatively warm temperature, a significant atmospheric mixed layer develops in this airmass by strong heating and moistening by the ocean (Kondo, 1976; Asai and Nakamura, 1978). Many shallow convective clouds with tops lower than several thousand meters above sea level (ASL) appear in the mixed layer. These clouds advect to southeast, and land at the west coast of the Japan Islands. These clouds are referred to as snow clouds because they provide snow over Japan. Over, and near Japan, the snow clouds are modified by topography. Snowfall activity is intensified windward of the divide of the islands around 1000 m or more ASL, and weakened in the lee due to orographic ascent and descent, respectively. Intensification of ice nucleation due to orographic ascent accompanying cloud-top-temperature decrease largely contributes to maintaining the observed active snowfall over the windward slope of the divide (Saito *et al.*, 1996). Climatological snow-depth is thus much larger in the windward side (the Japan Sea side), than in the lee side (the Pacific side) of the divide.

Between the Japan Sea and the divide, another several ridges exist intermittently over the islands. Climatological heavy snowfall is observed in many basins located between these low-altitude ridges with height of $\sim$ 500 m ASL and the divide (*e.g.*, Kodama *et al.*, 1995), and this suggests that these low-altitude ridges increase the amount of snowfall in their lee. Since the snow clouds are confined within a mixed layer capped with a stable layer, they are strongly affected by the depth change of the mixed layer over the ridges. According to a theory on flow regime of 2–D two-layer flow passing over a ridge (Saito, 1992), the top of the mixed layer is heightened (lowered) in a supercritical (subcritical) regime when the Froude Number is more (less) than one. In analyses of single Doppler radar observations of the snow clouds passing over the Dewa Hills ($\sim$ 38.7°N, $\sim$ 140.0°E) with average height of 600 m, Nakai *et al.* (1990) showed a case of the supercritical regime when the snow clouds extended upward above the Dewa Hills, while Nakai and Endoh (1995) showed a case of the subcritical regime when the tops of the snow clouds were lowered above the hills.

From a theoretical perspective, Saito (1992) demonstrated that a 2–D ridge in a 2–D flow induces a partial blocking upstream from the ridge. Pierrehumbert and Wyman (1985) showed that wind deceleration due to a partial blocking by a ridge continuously propagates upstream under non-rotating conditions and stagnates by keeping a constant distance from the ridge under the influence of the Coriolis force. This blocking maintains updraft which intensifies convective clouds over the upstream regions. Saito *et al.* (1994) and Kanada *et al.* (1999) pointed out that a blocking of low-level flow by the mountains of the Kii Peninsula ($\sim$ 34°N, $\sim$ 136°E) intensified the convective clouds over the upstream ocean. Fujiyoshi (1992) suggested that a large amount of climatological snowfall observed over Mt. Gassan ($\sim$ 38.5°N, $\sim$ 140.0°E) facing the Japan Sea, is partly ascribed to the intensification of the snow clouds by a partial blocking over the upstream ocean. However, the behavior of the snow clouds and airflow in the upstream of low-altitude ridges has not been well investigated, due to lack of observational studies.

The main purpose of this study is to investigate the behavior of the snow clouds and airflow passing over the Tsugaru mountains, which is a low-altitude ridge of 200 to 700 m ASL facing the Japan Sea. We analyze the data from a special field experiment performed over the Tsugaru district (Fig. 1), a heavy snowfall area in Japan, using single Doppler radar observations and rawinsondes. Since the radar observation circle covers both the upstream and downstream regions of the Tsugaru mountains, we can describe the behavior of the snow clouds and airflow passing over the Tsugaru mountains and discuss the dynamic effect of a low-altitude ridge on the snow clouds and airflow. High-altitude mountains also exist in the observation circle (Fig. 1), which allows the influence of these mountains on the snow clouds and airflow to be studied.

Although this paper is a case study, we show climatological features of snowfall activity and surface wind in Aomori Prefecture as a reference to examine our results. The Tsugaru district is the western portion of Aomori Prefecture. Figure 2 shows the long-term averaged fields of annual maximum snow depth, and the surface airflow pattern when the winter monsoon prevailed (Nibe, 1989). The mean maximum snow depth was derived from observation data for 20- or 30-year-long continuously obtained at agricultural meteorology observatories before 1974, and at the stations of Automated Meteorological Data Acquisition System (AMeDAS) after 1974. The mean surface airflow pattern was derived from about 10-year-long data of the most frequent wind direction at the AMeDAS stations. The AMeDAS is an operational meso-scale observation net work of Japan Meteorological Agency (JMA). Values of large snow depth appear over the windward slopes of the Hakkouda and Shirakami mountains and also in a zone extending over the plains passing the three AMeDAS stations; Goshogawara, Aomori, and Noheji. This zone of increased snow depth is located to the north of the Hakkouda mountains and is maintained by a climatological wind convergence zone (Fig. 2). North-westerlies from the Japan Sea converge with westerlies deflected around

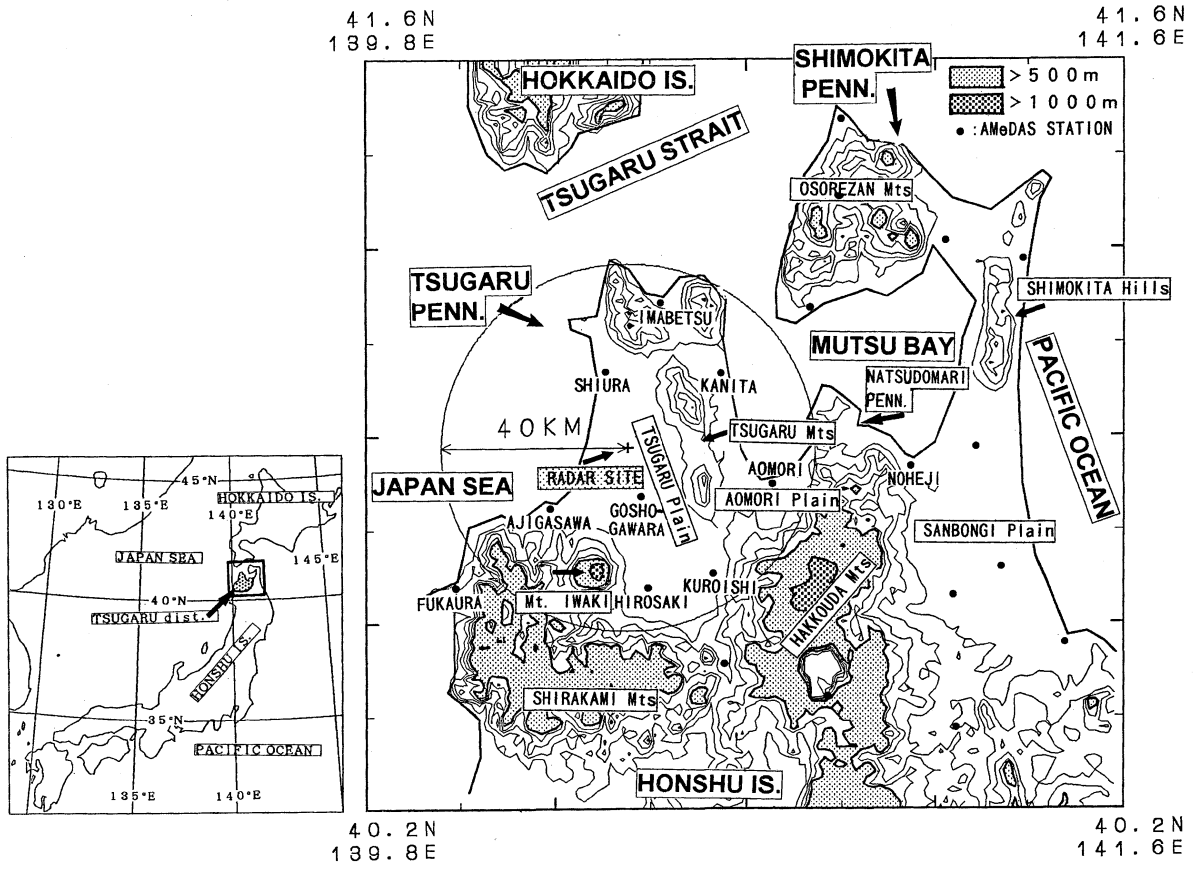

Fig. 1. Position of the study area (the Tsugaru district) (left panel) and topography and place names around the study area (right panel). The radar observation area is shown by an open circle. Light (dark) shadings indicate the regions with altitude higher than 500 m (1000 m) ASL.

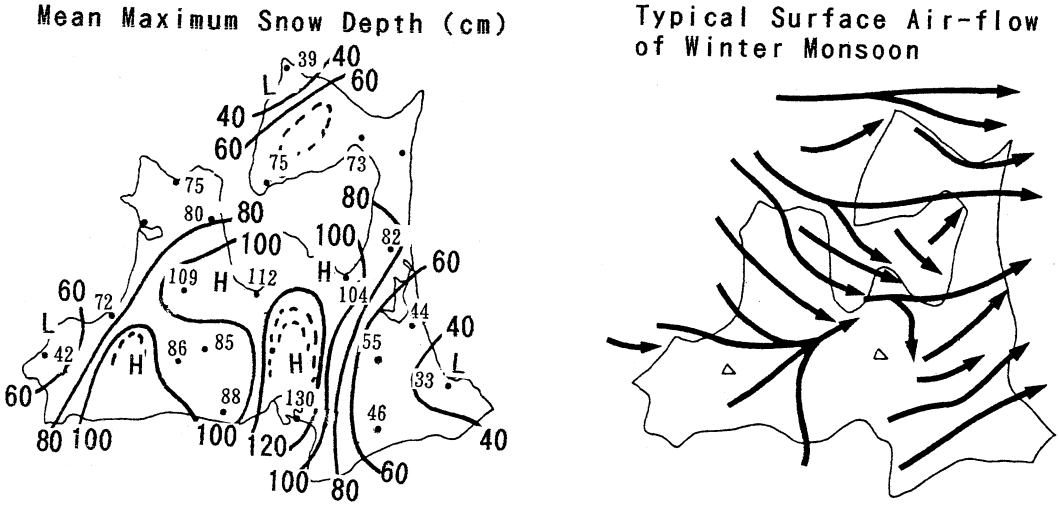

Fig. 2. Climatological maximum snow depth during winter (left panel) and mean surface airflow pattern when the winter monsoon is prevailing (right panel) over Aomori Prefecture (after Nibe 1989).

the Shirakami mountains and Mt. Iwaki, and southwesterlies prevailing over the Aomori plain and the southern portion of the Tsugaru plain (Nibe, 1989; Rikiishi and Hayashi, 1994, 1995). We will show that our results are almost consistent to these climatological features, except for several differences.

In Section 2, the observation systems and data processing method utilized in this study are described. In Section 3, we survey the synoptic situation and general aspects of the snow clouds and airflow in the observation area. The process to specify our main study period (1203–1747 JST[1] 25 Jan.

1 Japan Standard Time; GMT + 0900

1990) is also shown. In Section 4, the orographic effect of the Tsugaru mountains on the snow clouds and airflow is studied, and our results are compared to a theoretical prediction of 2–D two-layer flow passing over a ridge. In Section 5, we discuss a possible cloud-physical process in the snow clouds affected by the Tsugaru mountains, and possible formation mechanisms of a significant snowfall zone which developed over the central portion of the Tsugaru plain. Section 6 presents a summary and a remark.

2. Verification of observation data and data processing methods

An intensive field experiment was performed in the Tsugaru district by the National Research Institute for Earth Science and Disaster Prevention (NIED) during late January 1990, as a part of NIED's project to clarify the mechanisms of severe blizzards observed over the Tsugaru plain (Higashiura, 1990; Maki *et al.*, 1992). The radar site was placed near the center of the Tsugaru plain approximately 15 km to the west of the Tsugaru mountains (Fig. 1). The maximum range of the radar was 40 km and the radar site was chosen so that the snow clouds and airflow could be observed in both the upstream and downstream regions of the Tsugaru mountains. One exception was the low-level atmosphere around Mutsu Bay where the radar beam was interrupted by the Tsugaru mountains. Three-hourly low-level rawinsonde observations (up to around 4000 m above the ground level; AGL) were recorded at the radar site and supplemented by hourly observations of surface air temperature and wind at the AMeDAS stations in Aomori Prefecture. Positions of the AMeDAS stations are shown in Fig. 1.

The radar utilized for the observation period is an X-band Doppler radar of NIED. The observational resolution is 250 m in range and one degree in azimuth. This radar takes around 4 minutes to complete one CAPPI mode scan composed of 19 PPI scans while decreasing the elevation from 21.6° to 0.6°. A comprehensive report on the operational details of the radar can be found in Maki *et al.* (1989). During the main study period, CAPPI, RHI, and other mode scans were periodically performed at 6 to 10 minutes. The data of the CAPPI mode scan is processed to obtain the 3–D fields of snowfall intensity, wind, and horizontal wind divergence. The Doppler velocity at the zenith observed by the RHI mode scan was also utilized to evaluate the fall velocity of precipitation particles.

Radar reflectivity is translated to snowfall intensity following a Z–R relationship proposed by Fujiyoshi *et al.* (1990) for snowfalls:

$$Z = 554.0 \times R^{0.89}, \tag{1}$$

where Z is radar reflectivity (mm^6 m^{-3}) and R is snowfall intensity (mm hr^{-1}). The minimum radar reflectivity detectable at the border of the observation volume was 15 dBZ, which corresponds to a snowfall intensity of 0.04 mm hr^{-1} from Eq. (1).

The horizontal wind and its divergence are evaluated by using the modified Volume Velocity Processing (MVVP) method proposed by Koscielny *et al.* (1982). In 3–D Cartesian coordinates, the MVVP method is applied to the Doppler velocity data within a small sub-volume centered at the point (x_0, y_0, z_0) where the wind and its derivatives are derived. When applying the MVVP method, linear variation of wind within the sub-volume is assumed, *i.e.*,

$$\begin{aligned} u &= u_0 + u_x(x - x_0) + u_y(y - y_0) + u_z(z - z_0) \\ v &= v_0 + v_x(x - x_0) + v_y(y - y_0) + v_z(z - z_0), \end{aligned} \tag{2}$$

where $u_x = \frac{\partial u}{\partial x}$, $v_y = \frac{\partial v}{\partial y}$, *etc.* Seven parameters, (u'_0, v'_0, $(u_y + v_x)$, u_x, v_y, u_z, v_z) are evaluated for the small volume by fitting a linear function of these parameters to the Doppler velocity data using a least-squares fit method. Here,

$$u'_0 = u_0 + y_0(v_x - u_y)/2$$

and

$$v'_0 = v_0 - x_0(v_x - u_y)/2, \tag{3}$$

show how the estimated horizontal wind components (u'_0 and v'_0) are contaminated by vorticity. Eq. (3) indicates that the contamination appears only in tangential wind component perpendicular to the radar beam, and becomes weaker with decreasing range from the radar site. Non-linear wind variations within the small volume will adversely affect the estimation using the MVVP method. According to Sasaki *et al.* (1998), the effect of non-linear variations to the estimation of horizontal wind and its divergence by the MVVP method is negligible (significant) when the non-linearity is less (greater) than 10^{-7} m^{-1}s^{-1}.

Koscielny *et al.* (1982) recommended the sub-volume to be composed of multiple planes of at least 30° times 20 km extension in azimuth and range directions, respectively, for evaluation of horizontal wind divergence with an accuracy of 10^{-5} s^{-1}. To describe the meso-scale wind structure at the 10 km scale, we reduced the extension of the sub-volume to be 30° (20°) times 8 km at the range from the site less (greater) than 25 km, and to be composed of three subsequent PPI planes within 2.4° in elevation. Since the accuracy of the estimation depends more upon the azimuthal width than the range of the sub-volume (Koscielny *et al.*, 1982), we can expect reasonable accuracy within a circle of 25 km range, but need to consider reduced reliability at larger ranges. Profiles of wind, and wind divergence

above the site, were evaluated by the Velocity Azimuth Display (VAD) method using the Doppler velocity data on the PPI plane at the maximum (21.6°) elevation. Wind estimation by the MVVP and VAD methods was confined to below 2500 m AGL due to the sparsity of available Doppler velocity data above 2500 m AGL. Before applying the MVVP and VAD methods, the Doppler velocity was compensated for the effect of gravitational falling of precipitation particles. The fall velocity was assumed to be 1.3 m s^{-1}, which was the mean Doppler velocity at the zenith observed by the RHI mode scan vertically averaged within the cloud layer, and temporally averaged for the main study period (not shown).

Within the observation volume, 3–D Cartesian coordinates were defined. Horizontal position is described by the distance from the radar site projected to each coordinate, for example (0, 0) and (20E, 15S) indicate the radar site, and the position 20 km to the east and 15 km to the south from the site, respectively. Vertical position is defined by the height AGL at the radar site. The grid-point interval for describing the snowfall intensity is 250 m horizontally and vertically to match with the radar observation resolution in range. Resolution of wind-field evaluation is determined by spatial extension of the sub-volume for applying the MVVP method. We adopted a horizontal grid-point interval of 5 km, and a vertical one of 500 m for describing the wind field to match with the horizontal and vertical extensions of the sub-volume at the range of 12 km from the site. Note that the resolution for the wind fields exceeds the grid-point interval at the range of more than 12 km.

Spurious results are sometimes derived by the MVVP method for several reasons. For example, noises in the Doppler velocity data, including convective-scale wind variation whose horizontal scale is smaller than the sub-volume, and non-linear wind variation in the sub-volume (Koscielny *et al.*, 1982; Sasaki *et al.*, 1998). To maintain the accuracy of our evaluation using the MVVP method, we took the following procedures: 1) the evaluation was not made for the sub-volume where the Doppler velocity data were partially distributed, *i.e.*, few data existed in either one of the three-divided sectors of the sub-volume; 2) evaluated values were not utilized for further analysis when the residual variation of the least-squares fitting of the MVVP method exceeded 2.0 m s^{-1}, because this large residual variation suggests the existence of strong non-liner wind variation or erroneous data in the sub-volume (Koscielny *et al.*, 1982; Tatehira *et al.*, 1998). The threshold value of 2.0 m s^{-1} was chosen following Tatehira *et al.* (1998), who showed that the residual variation exceeded 4.0 m s^{-1} and remained $\sim$ 1.0 m s^{-1} in sub-volumes with and without shear lines of strong non-linear wind variation, respectively, in their case study; 3) to exclude abnormally large or small evaluated values, the evaluated values of 20 % higher order and 20 % lower order were removed for each grid point. After that, the evaluated values were averaged for the main study period to remove the short period variation of the values (shown later).

In spite of the careful treatment shown above, the evaluated fields of wind and wind divergence should be interpreted with the following caveats: 1) The evaluation might be influenced by non-linear wind variation caused by the complex terrain around the study area. Although the influence of strong non-linearity was excluded by monitoring the residual variation of the least-squares fit method, the influence of moderate non-linearity may still remain in the evaluations; 2) Reliability of the evaluation may be low in the NNW and SSE sectors of the study area, where the absolute value of Doppler velocity was small due to the radar beam being perpendicular to the mean wind. Small Doppler velocity reduces signal-noise ratio, and hence decreases the reliability of the evaluation; 3) Reliability of the evaluation may decrease with increased range from the radar site. This is due to contamination of the evaluated wind field by vorticity, which is larger as the range is increased (Eq. (3)), and also due to azimuth extension of the sub-volume was reduced from 30° to 20° at the range exceeding 25 km; 4) Reliability of the evaluated wind is lower in the tangential component of wind than in the radial one. Both the non-linear wind variation and vorticity contamination would have stronger effect on the evaluated wind in the tangential component (Sasaki *et al.* (1998) and Eq. (3)).

Figure 3 shows temporal variation of the wind evaluated by the MVVP method at 1000 m AGL averaged over the eight grid points surrounding the radar site (lines) to be compared to the sonde-observed wind above the site at every three hours (capitals). In spite of the size difference of observation volume between the MVVP method and the rawinsondes, the evaluated wind and the observed wind are in good agreement, with the exception of the short period fluctuations in the evaluated wind speed. Similar agreement was confirmed at the other levels using the MVVP method and between winds evaluated by the MVVP method and by the VAD method (not shown). Random errors of the wind evaluation by the MVVP method (Tatehira and Suzuki, 1994), and convective-scale wind variation are possible causes of the short period fluctuation of the evaluated wind speed. Hereafter we will show only temporally-averaged wind fields to remove any influence of the short-period fluctuations.

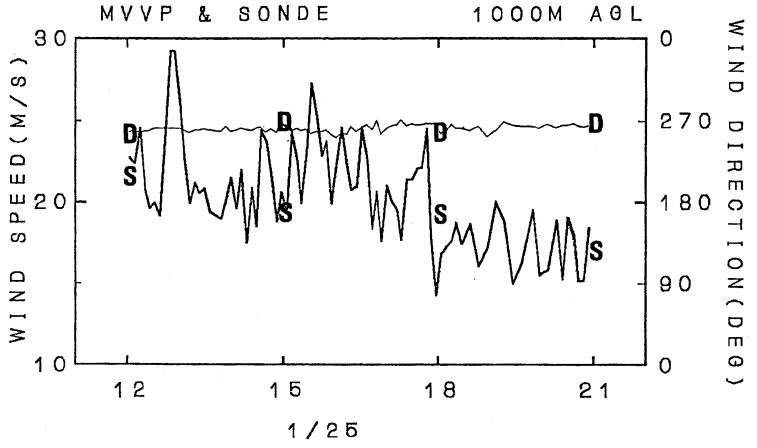

Fig. 3. Wind direction (D) and wind speed (S) at 1000 m above the radar site obtained by three-hourly rawinsonde observations between 12 JST 25 and 03 JST 26 Jan. 1990. The thin (thick) line indicates the temporal variation of wind direction (wind speed) at 1000 m above the radar site derived from a single Doppler radar observation using the MVVP method.

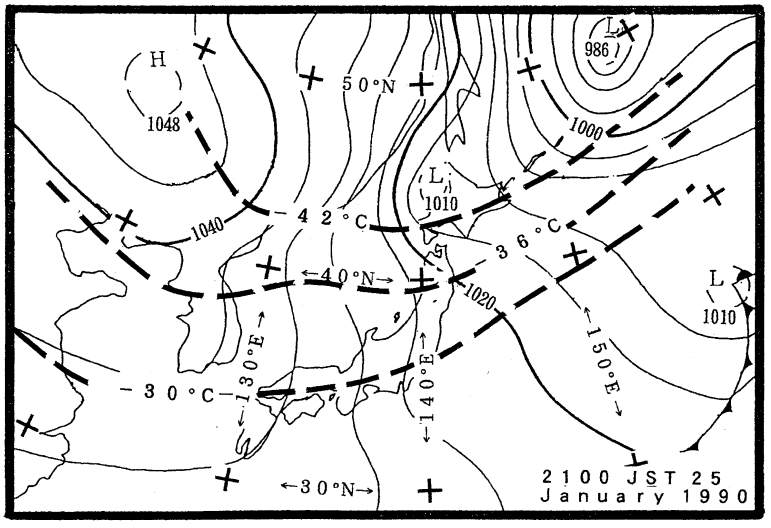

Fig. 4. Sea-level pressure (solid contours at 4 hPa intervals) and 500 hPa temperature (dash contours at 6°C intervals between −30°C and −42°C) over East Asia at 2100 JST 25 Jan 1990.

3. Synoptic situation, general aspects of snowfall activity and airflow over the study area, and process to specify the main study period

In the intensive observation period, a winter monsoon prevailed between 23 and 28 Jan. 1990. The low-level air temperature at the radar site was coldest during the period from 1200 JST 25 to 0300 JST 26 Jan. 1990. We concentrate our analysis on the main study period of 1203–1747 JST 25 Jan. The reason to specify the main study period will be shown later in this section.

Synoptic fields of sea-level pressure (SLP) and 500 hPa temperature at 2100 JST 25 Jan. 1990, just after the main study period of 1203–1747 JST 25, are shown in Fig. 4. A strong east-west SLP gradient developed near Japan between a strong cyclone over the North Pacific, and an anticyclone over Siberia. Although this was similar to the climatological large-scale SLP pattern when the winter monsoon prevails around Japan, contours of SLP around the study area were oriented not N–S as in the climatology but NW–SE due to a small depression on the west coast of Hokkaido Island. Surface wind direction thus veered somewhat northward from climatology over the study area (shown later). The 500 hPa temperature was ~ 5°C colder than climatology around the northern part of Japan, which indicates an intrusion of a strong cold polar airmass.

Figure 5 shows mean surface wind and surface air temperature at the AMeDAS stations in Aomori Prefecture averaged over the 6-hr period between 1200 and 1800 JST 25 Jan. Surface air temperature was much colder than the freezing point and all precipitation particles over the study area were in ice phase. Wind direction was WSW at Ajiga-

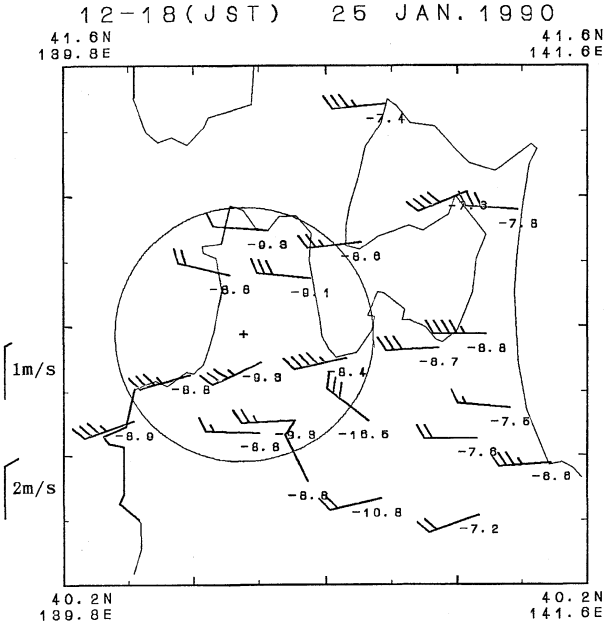

Fig. 5. Mean surface wind and temperature (°C) in Aomori Prefecture observed at the AMeDAS stations averaged over the period of 1200–1800 JST 25 Jan. 1990. Each full barb and half barb indicate 2 m s^{-1} and 1 m s^{-1}, respectively. A large open circle indicates the radar observation area.

sawa, Goshogawara, and Aomori in the southern portion of the observation area, while it was W to WNW at Shiura and Kanita in the northern portion. This indicates the existence of a convergence zone passing over the central portion of the Tsugaru plain. Later we will show that snowfall was intensified along this convergence zone. A similar convergence zone is found in the climatological wind field when the winter monsoon prevails (Fig. 2), although the wind direction for this study veered somewhat northward from the climatological one and the SW wind over the southern part of the Tsugaru plain was not observed.

Figure 6 shows the temporal variation of wind and potential temperature profiles observed by low-level rawinsondes three-hourly launched at the radar site between 00 JST 25 and 12 JST 26 Jan. 1990. A mixed layer of about 3000 m depth capped by a strong stable layer was observed. Thickness of the mixed layer exceeds any mountain height in and around the observation area. Before 1800 JST 25, a WSW wind dominated both in and out of the mixed layer, while a W to WNW wind appeared in the mixed layer after 2100 JST 25 Jan. Wind speed was 15–20 m s^{-1} within the layer and 20–50 m s^{-1} out of the layer, although it decreased gradually. As shown by the contour of 264 K of potential temperature, surface air temperature was lowest during the 15-hour period between 1200 JST 25 and 0300 JST 26 Jan. 1990.

Within this 15-hour period of the lowest temperature, we specified the main study period to be between 1203 and 1724 JST 25 Jan. to satisfy the following conditions: 1) The snow clouds were widely observed over the study area; 2) Wind speed and wind direction were nearly constant with time; 3) Meso-scale disturbances, which sometimes develop over the Japan Sea (*e.g.*, Kodama *et al.*, 1995), did not appear in the vicinity of the study area.

The first condition is necessary for applying the MVVP method, because the Doppler velocity was observed only in the snow clouds in our case. Figure 7 shows temporal variation of snowfall intensity at 1000 m AGL along a N–S oriented line at 20W over the Japan Sea. The snow clouds were widely distributed and concentrated around 20S and 10N, before and after an observation interruption between 2055 and 2152 JST 25 Jan. Since the MVVP method can not be applied to the broad cloud-free region of 0–20S, we excluded the period after 2055 JST 25 Jan. from the main study period. Unfortunately, the snow clouds scarcely appeared throughout the period over the southern portion of the Tsugaru plain in the lee of the high-altitude mountains, where reliable evaluations by the MVVP method were not abundant. The second condition is necessary to take a temporal average of the evaluated wind to remove the short-period fluctuations of the evaluated wind (Fig. 3). Aside from the short-period fluctuations, wind speed and wind direction evaluated by the MVVP method were almost constant between 1203 and 1747 JST 25, while wind speed decreased and wind direction veered southward gradually with time after 1747 JST 25 (Fig. 3). We thus excluded the period after 1747 JST 25. The third condition is necessary to study orographic effects on the snow clouds in an airflow free from the influence of meso-scale disturbances. We confirmed that no significant meso-scale disturbances existed in the vicinity of the study area between 1203 and 1747 JST 25 by an operational weather-radar observation at Hakodate (~ 42°N, ~ 141°E) covering the study area and offshore ocean (not shown). Finally, the main study period was fixed between 1203 and 1747 JST 25 Jan. 1990.

Figure 8 shows the mean field of snowfall intensity at 1000 m AGL averaged over the main study period. The snowfall field at 1000 m AGL was chosen in spite of possible development of snow particles below this level, because the area where the radar beam was interrupted by mountains increases with decreasing the height of level. Snowfall intensity fields at 500 m and 1000 m AGL showed qualitatively similar features over the observable areas (not shown). Snowfall intensity over the Tsugaru plain, and the Japan Sea, was stronger in the upstream of the corridors of the Tsugaru mountains

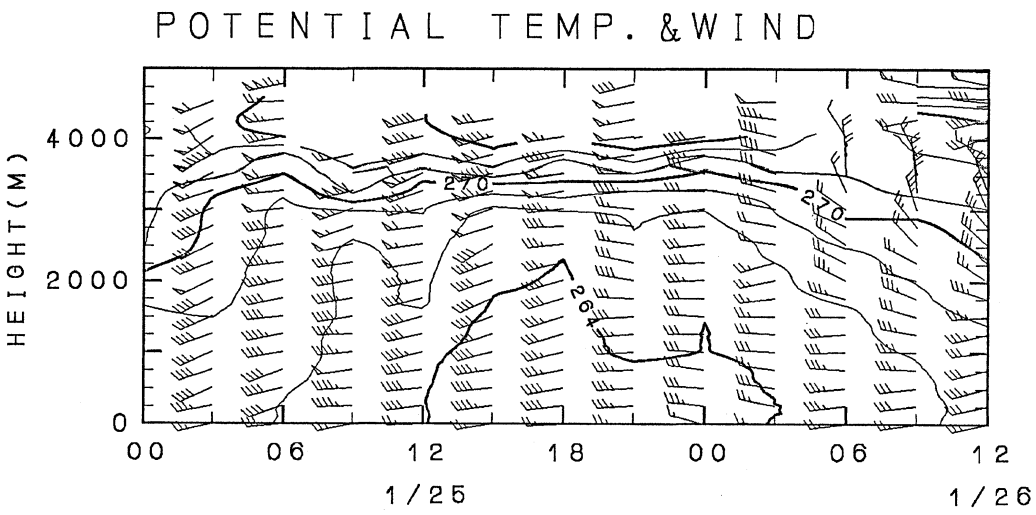

Fig. 6. Time-height cross-section of potential temperature (solid contours at 2 K intervals) and horizontal wind (barbs; each pennant and barb indicate 25 m s^{-1} and 5 m s^{-1}, respectively) derived from rawinsonde observations at the radar site for the period between 0000 JST 25 and 1200 JST 26, Jan. 1990.

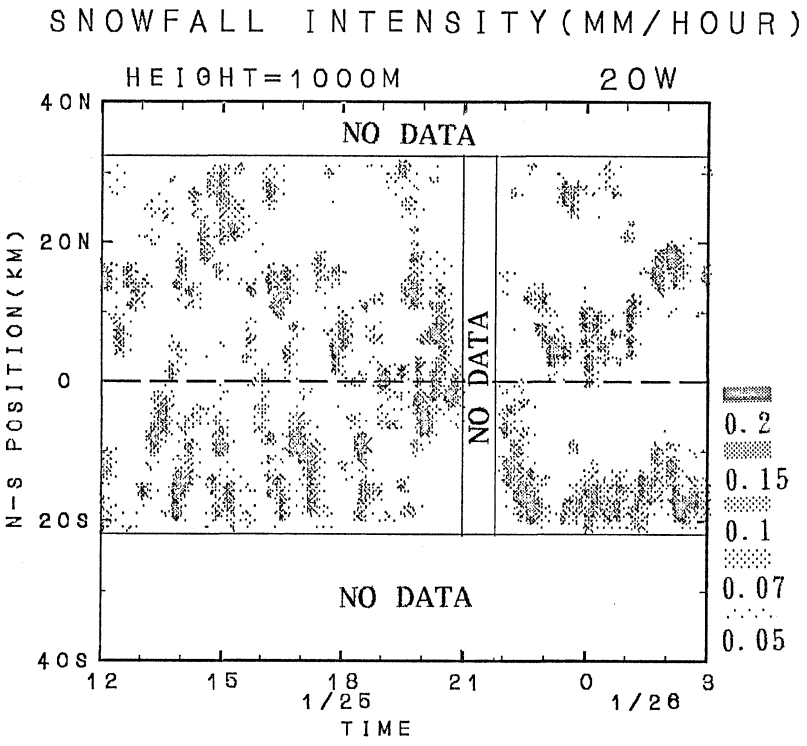

Fig. 7. Temporal variation of snowfall intensity (mm hr^{-1}) at 1000 m AGL between 1200 JST 25 and 0300 JST 26 Jan. 1990 along a N–S oriented line over the Japan Sea at 20W. No data are shown between 2055 and 2152 JST 25 when the CAPPI mode scan was stopped, to the south of 21S where snowfall intensity could not be evaluated by ground scattering, and to the north of 33N, which was out of the radar range.

($\sim$ 20N, $\sim$ 10E, and $\sim$ 0, $\sim$ 15E), and weaker in the upstream of the peaks of the mountains ($\sim$ 25N, $\sim$ 0, and $\sim$ 10N, $\sim$ 12E). An intensified snowfall zone extended between the Japan Sea on the north of the Shirakami mountains and Mutsu Bay passing through the central corridor of the Tsugaru mountains ($\sim$ 0, $\sim$ 15E). The intensified snowfall along this zone was sustained by the consequent passage of the snow clouds along the zone (not shown). The snowfall zone extended along the wind convergence zone at the surface (Fig. 5). A zone of negligible snowfall appeared in the lee of the Shirakami moun-

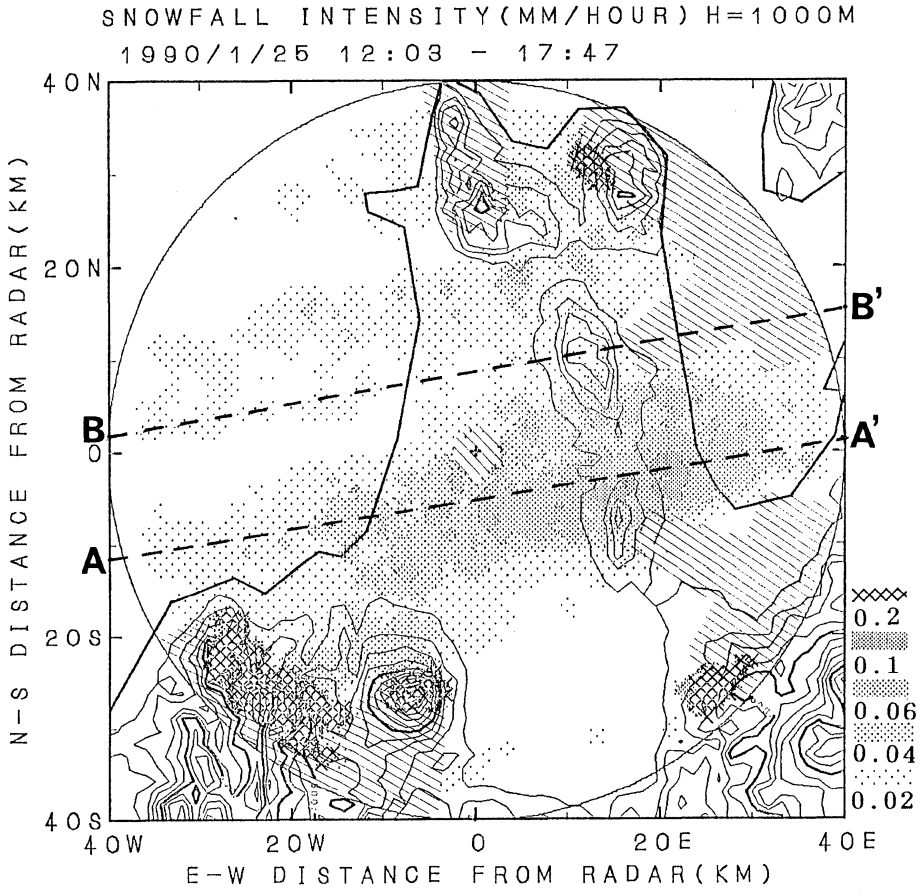

Fig. 8. Mean snowfall intensity (mm hr^{-1}) at 1000 m AGL averaged over the main study period of 1203–1747 JST 25 Jan. 1990 (shading) and topography (contours at 100 m intervals). The regions above the radar site and in the shade of mountains, where no radar observations were taken, are lightly hatched. Cross-hatched areas correspond to ground scattering. Two dashed lines indicate the positions of cross-sections shown in Fig. 15.

tains, and Mt. Iwaki, and extended eastward for more than 40 km toward the Aomori plain.

Figure 9 shows horizontal wind (vectors) and wind speed (contours with shading) at 1000 m AGL averaged over the main study period derived by the MVVP method. The dominant wind direction was W or WSW in most of the observation area, and wind speed was small over the southern portion of the Tsugaru plain in the lee of the Shirakami mountains and Mt. Iwaki. A weak-wind zone extended over the central and northern portions of the Tsugaru plain parallel to the Tsugaru mountains around 15 km upstream of the mountains. In this zone, wind speed was 2 to 4 m s^{-1} weaker compared to either side. This weak-wind zone was parallel not to the coast line of the Japan Sea, but to the crest of the Tsugaru mountains. This suggests that not land-sea roughness difference, but the dynamic effect of the Tsugaru mountains, was important in the formation of the weak-wind zone. Mechanisms of this dynamic effect will be examined further in Section 4.

Figure 10 shows the divergence of the horizontal wind at 1000 m AGL derived by the MVVP method averaged over the main study period. Strong wind convergence and divergence appeared along the western and eastern edges of the weak-wind zone, parallel to the Tsugaru mountains. This convergence and divergence was qualitatively consistent with the wind speed variation across the weak-wind zone, because the wind speed variation along the western and eastern edges of the weak-wind zone was 2–4 m s^{-1} over a distance of 5–10 km (Fig. 9), which corresponds to a wind divergence or convergence of the order of 10^{-4}–10^{-3} s^{-1}, consistently with the values shown in Fig. 10. Strong wind convergence was also observed along a WSW-ENE oriented zone in the central portion of the Tsugaru plain. This convergence zone corresponded to the snowfall zone found in Fig. 8. Weak wind divergence appeared on the north of this convergence zone, where the mean snowfall intensity was relatively weak (Fig. 8).

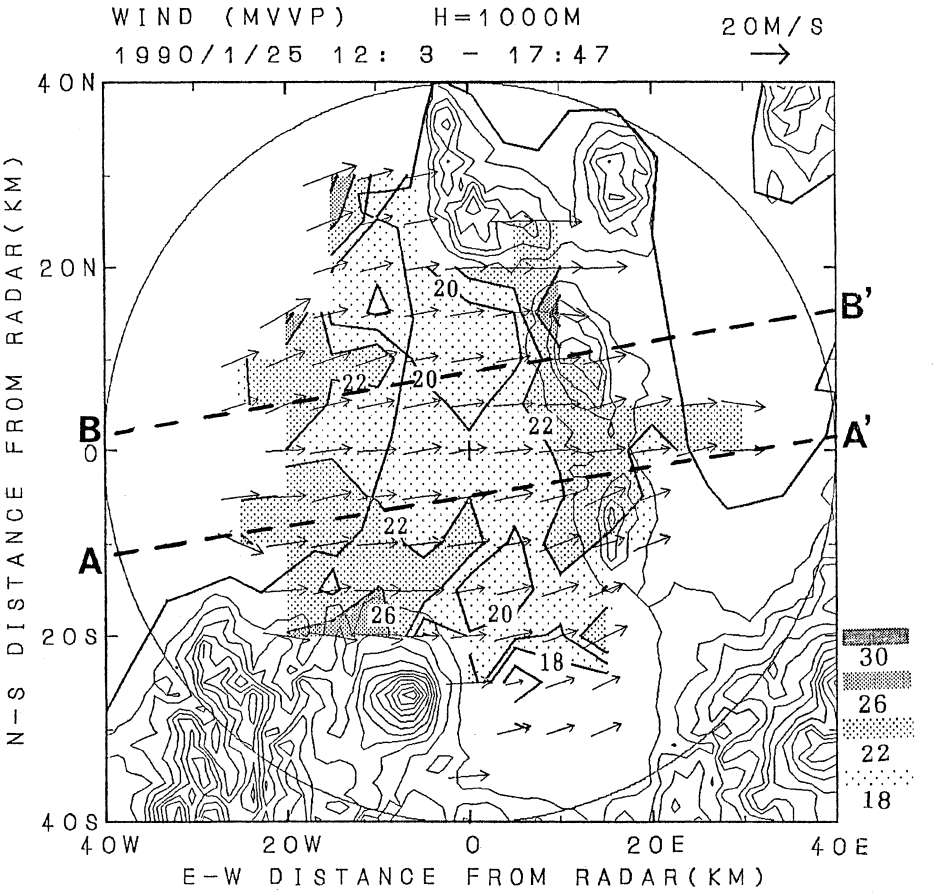

Fig. 9. Same as in Fig. 8 except for mean horizontal wind (vectors) and wind-speed (contours at 2 or 4 m s^{-1} intervals with shading) at 1000 m AGL averaged over the main study period. No vectors are shown in the regions where reliable wind estimation could not be obtained using the MVVP method.

4. Analysis of the behaviors of the airflow and the snow clouds passing over the Tsugaru mountains

4.1 Confirmation of the weak-wind zone in the upstream of the Tsugaru mountains

In the preceding section, we found a weak-wind zone extending parallel to the Tsugaru mountains around 15 km upstream of the mountains (Fig. 9). However, this weak-wind zone requires further examination, because it extended to the NNW and SSE sectors where the reliability of wind evaluation by the MVVP method was low due to near-zero Doppler velocity, as remarked in Section 2.

First, the wind-speed variation was examined across the weak-wind zone along a line directed at 260° parallel to the mean wind and passing over the radar site. Figure 11 shows the wind speed evaluated by the MVVP method (the VAD method above the radar site) (solid line) along the above defined line, averaged over the main study period. High reliability of the evaluated wind speed can be expected along this line, since signal-noise ratio was high, because of large absolute values of the Doppler velocity. The evaluated wind speed was not affected by the less reliable tangential component of the evaluated wind (*cf.*, Section 2). Figure 11 also shows the absolute value of Doppler velocity (dots) along the line on a PPI plane of 2.4° elevation averaged over the same period. The Doppler velocity on a low elevation plane almost agrees with the real wind speed along the line parallel to the mean wind. Since the height of the PPI plane changed with range from the site, the evaluated wind speed by the MVVP method on the level closest to the PPI plane is shown for comparison to the Doppler velocity, except within the 14 km in range, where the evaluated wind speed at 500 m AGL is shown.

The Doppler velocity and evaluated wind speeds were in good agreement with each other. Both data indicate that wind speed was clearly diminished around the radar site within a $\sim$ 20 km width. A part of the decrease in the Doppler velocity near the site where the PPI plane approached the ground surface may be ascribed to a frictional deceleration of the wind near the surface. The frictional effect seems to be confined within 5 km in range because the wind-speed decrease was confined near the surface according to sonde observations. Fig. 12 shows the mean profiles of sonde-observed wind speed and

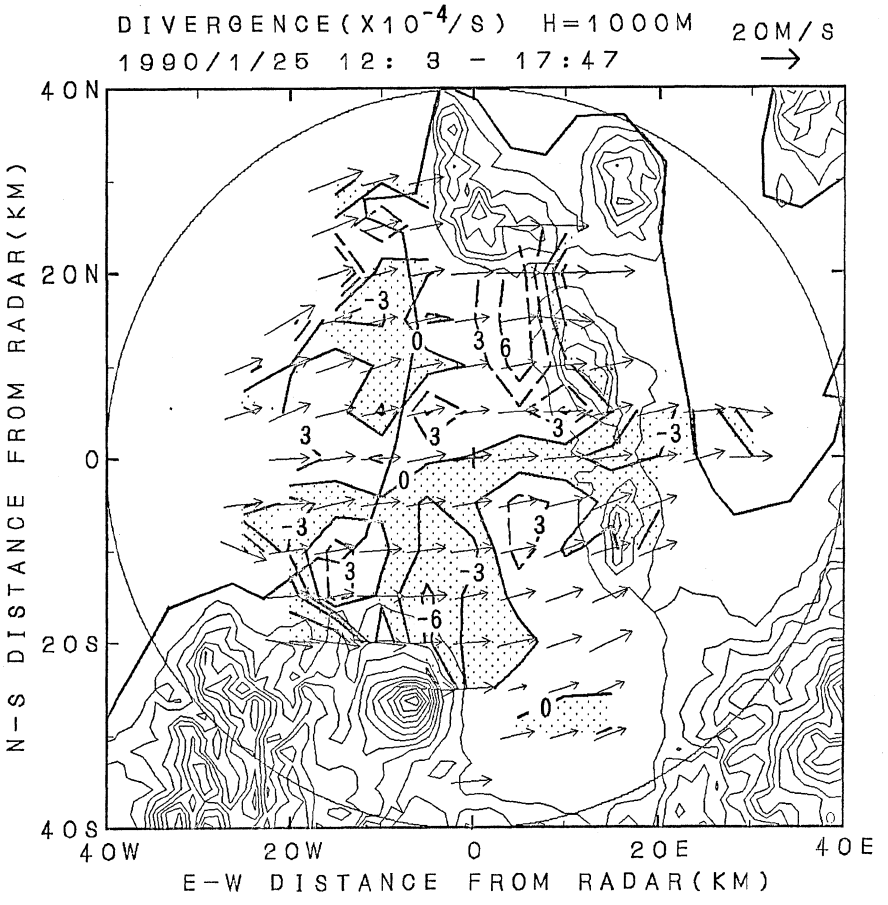

Fig. 10. The same as in Fig. 9 except for wind divergence (contours at 3×10^{-4} s^{-1} intervals with shading below zero).

potential temperature at the radar site averaged over the main study period. The wind speed was relatively constant between 200 m and 2500 m AGL, and the frictional wind-speed decrease was significant below 200 m AGL. Since 200 m AGL on the PPI plane of 2.4° elevation corresponds to 5 km in range from the site, the reduced Doppler velocity around the site out of 5 km in range indicates the existence of the weak-wind zone. The results shown in Fig. 11, therefore, confirm the existence of the weak-wind zone, at least on the line parallel to the mean wind and passing over the radar site.

To examine the weak-wind zone away from the radar site where the evaluated wind speed depends strongly on the less reliable tangential component of the evaluated wind, we investigated the advection speed of long-lasting snow clouds, because the speed of these clouds may reflect the wind speed averaged over the cloud layer. Figure 13 shows seven time-sequential fields of snowfall intensity at 1500 m AGL to track a long-lasting snow cloud which passed through the northern portion of the weak-wind zone. To show the advection speed of the cloud precisely, the vertical spacing of the panels is proportional to the temporal interval of each PPI scan which detected the tracked cloud around 1500 m AGL, because displacement of the cloud was not negligible within one CAPPI mode scan which took around 4 minutes. The eastward propagation speed of the cloud significantly decreased from $\sim$ 25 m s^{-1} to $\sim$ 20 m s^{-1} at 1421 JST 25 Jan. 1990. After 1432 JST, the speed increased to $\sim$ 23 m s^{-1} over the ridge. This change of the advection speed is consistent to the wind-speed variation across the weak-wind zone (Fig. 9). Similar deceleration and acceleration around the weak-wind zone was observed for other long-lasting clouds (not shown), although only a few clouds lasted from the Japan Sea to Mutsu Bay.

The weak-wind zone extended to the NNW-SSE sectors where the reliability of the evaluated wind by the MVVP method was low during the main study period. To confirm that the weak-wind zone shown in Fig. 9 was not a "ghost artifact" due to the reduced reliability of the wind evaluation, we examined the wind field evaluated by the MVVP method for an other period between 0000 and 0511 JST 26 Jan. 1990, when the mean wind direction was W to WNW, different from the main study period (Fig. 14). In spite of the directional change of the mean wind, a weak-wind zone appeared in the upstream of the Tsugaru mountains and extended

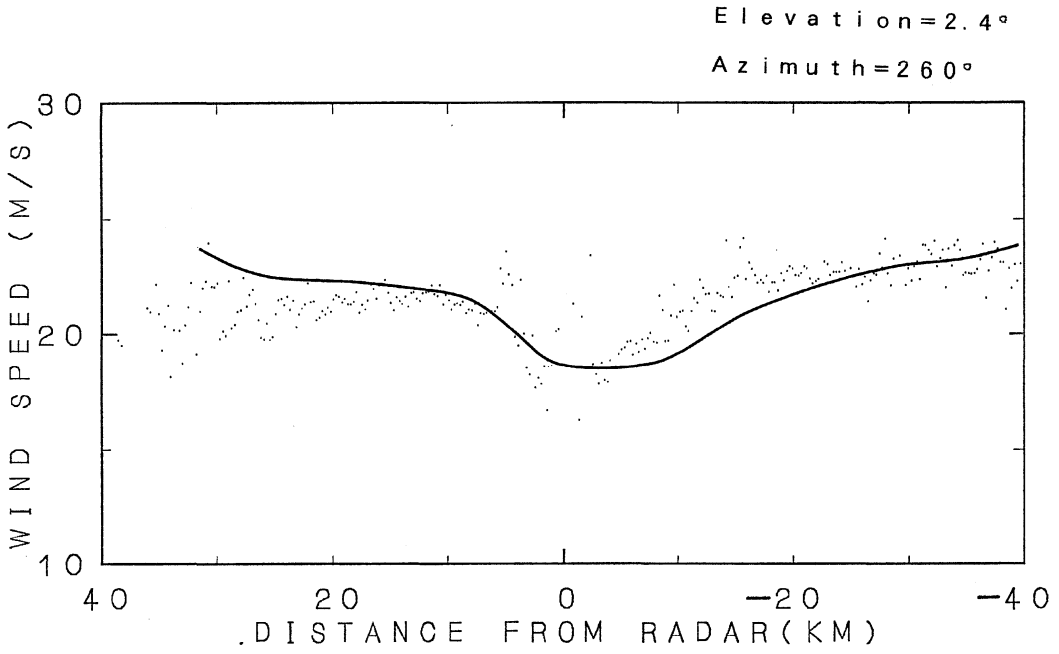

Fig. 11. Mean Doppler velocity (dots) and wind-speed estimated by the MVVP method (line) along a line passing through the radar site parallel to the mean wind averaged over the main study period. Both data were obtained on or close to a PPI plane of 2.4° elevation, however, the estimated wind-speed at 500 m AGL is shown within the range of 12.5 km.

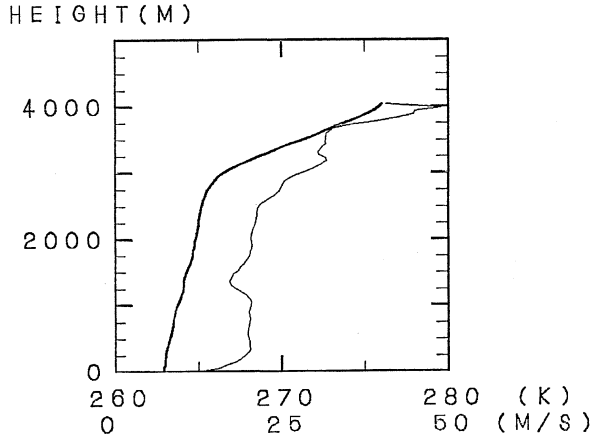

Fig. 12. Mean profiles of potential temperature (thick like) and wind speed (thin line) derived from the three-hourly rawinsonde observations at the radar site averaged over the period of 1200–1800 JST 25 Jan. 1990.

not to the sectors perpendicular to the mean wind, where the Doppler velocity was near-zero, but parallel to the Tsugaru mountains. This suggests that the weak-wind zone shown in Fig. 9 was real, and not due to spurious wind estimation.

We also examined the influence of non-linear wind variation around the weak-wind zone to the wind evaluation by the MVVP method. We define a dependable wind-speed variation across the weak-wind zone shown by a solid line in Fig. 11, where the absolute value of non-linearity exceeded $\sim 10^{-7}$ $m^{-1}s^{-1}$ at several points of strong curvature in the wind-speed variation (not shown). As introduced in Section 2, non-linear wind variation more than 10^{-7} $m^{-1}s^{-1}$ may lead to significant errors in the evaluation of wind (especially in the tangential component) and wind divergence by the MVVP method (Sasaki *et al.*, 1998). If we suppose a constant wind speed along the weak-wind zone, non-negligible errors might appear in the evaluations using the MVVP method around the weak-wind zone away from the site where the tangential component of the evaluated wind was large. Nevertheless, results shown in this subsection support the existence of the weak-wind zone.

4.2 The influence of a partial blocking by the Tsugaru mountains to snowfall activity

Wind speed variation across the weak-wind zone was accompanied with wind convergence and divergence along the western and eastern edges of the weak-wind zone. The snow clouds may be modified by vertical flow induced by this divergent wind, and thus we investigate snowfall activity around the weak-wind zone, and we discuss the relationship of the wind field to snowfall activity.

Figure 15 shows two vertical cross-sections of snowfall intensity and wind speed along two lines (A–A' and B–B' in Figs. 8 and 9), roughly parallel to the mean wind. One line (Fig. 15(a)) is along the snowfall zone passing around a corridor of the Tsugaru mountains, and the other (Fig. 15(b)) is located to the north of the radar site passing over a

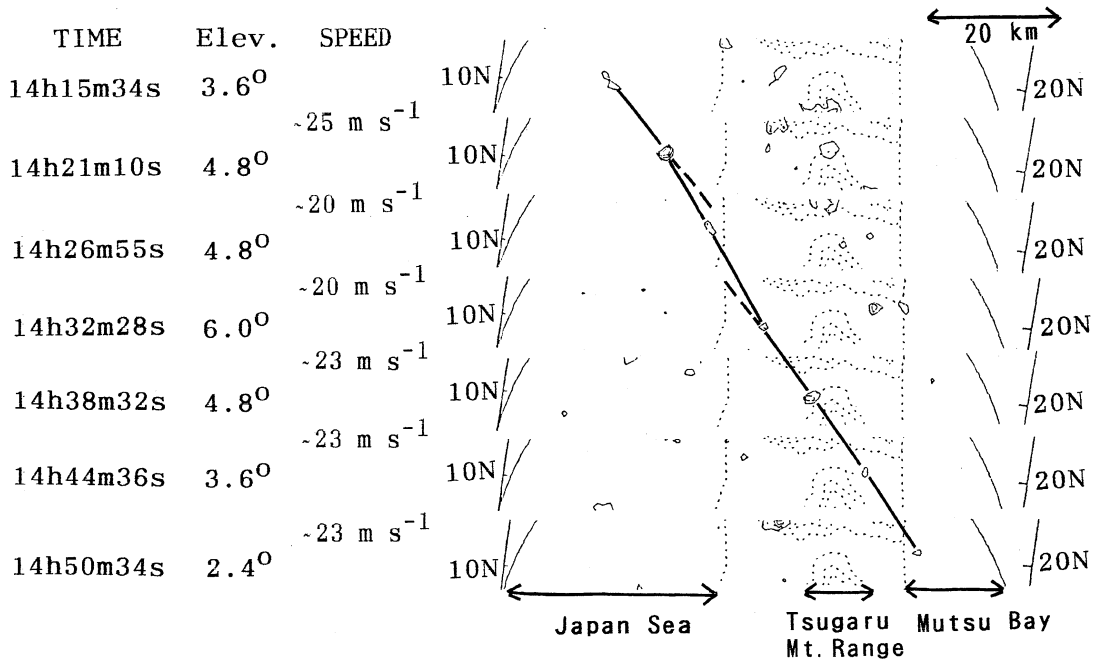

Fig. 13. Time sequence of an eastward-moving snow cloud during the period of 1415–1450 JST 25 Jan. 1990. Contour interval is 0.2 mm hr^{-1} of snowfall intensity at 1500 m AGL. Propagation of the target cloud is shown by thick lines. Time and elevation of the PPI scan detecting the target cloud at 1500 m AGL, and evaluated advection speed of the cloud are shown. Dotted lines indicate the coast line and height contours of topography at 100 m intervals.

peak of the Tsugaru mountains, as shown in Figs. 8 and 9. In both cross-sections, the tops of the snow clouds extended upwards 10 to 15 km upstream of the Tsugaru mountains, then descended steeply toward the east above and in the lee of the mountains, and finally ascended over Mutsu Bay. Wind speed was a minimum in the weak-wind zone about 15 km upstream of the mountains and increased in strength eastward above and in the lee of the mountains. The weak-wind zone was more obvious in the low-levels, but extended throughout the whole mixed layer. The cloud tops ascended (descended) around the western (eastern) edge of the weak-wind zone where wind speed decreased (increased) toward the east, accompanied with wind convergence (divergence).

The distribution of the maximum echo-top height (Fig. 16) was determined for each grid point during the main study period. The echo top was defined by the uppermost contour of 0.1 mm hr^{-1} of snowfall intensity. This threshold exceeded the minimum detectable snowfall intensity ($\sim$ 0.04 mm hr^{-1}) at the border of the observation area. The maximum echo-top height was largest around 15 km upstream of the Tsugaru mountains near the weak-wind zone, except over the southern portion of the Tsugaru plain where the snow clouds were rarely observed. The maximum echo-top height increased and decreased around the low-level convergence and divergence along the western and eastern edges of the weak-wind zone, respectively (Figs. 9 and 10). This confirms that the result shown in Fig. 15 was commonly observed over the central and northern portions of the Tsugaru plain and strongly suggests a dynamic link between the swelled snow clouds and the weak-wind zone in the upstream of the Tsugaru mountains.

Over the Tsugaru Plain, the echo-top might be detached from the top of the mixed layer due to gravitational falling of snow particles, because the interruption of heat supply from the Japan Sea after the landing of the snow clouds seemed to weaken the convection in the snow clouds. Over the Tsugaru plain, however, we can expect that the variation of the maximum echo-top height reflected the variation of the mixed-layer top. The reason is that the vertical extension of the snow clouds is confined to the tops of the mixed layer, and the top height of the mixed layer ($\sim$ 3000 m) observed by the sondes (Fig. 12) was close to the maximum echo-top height around the radar site (2750 $\sim$ 3000 m; Fig. 16). Therefore, the increase of the maximum echo-top height around the western edge of the weak-wind zone strongly suggests an upward extension of the mixed layer. Since convective-scale updraft was weakened after the landing of the snow clouds, a larger-scale updraft whose horizontal extension exceeds the convective-scale updraft was necessary to sustain the upward development of the mixed layer. Wind convergence along the western edge of the

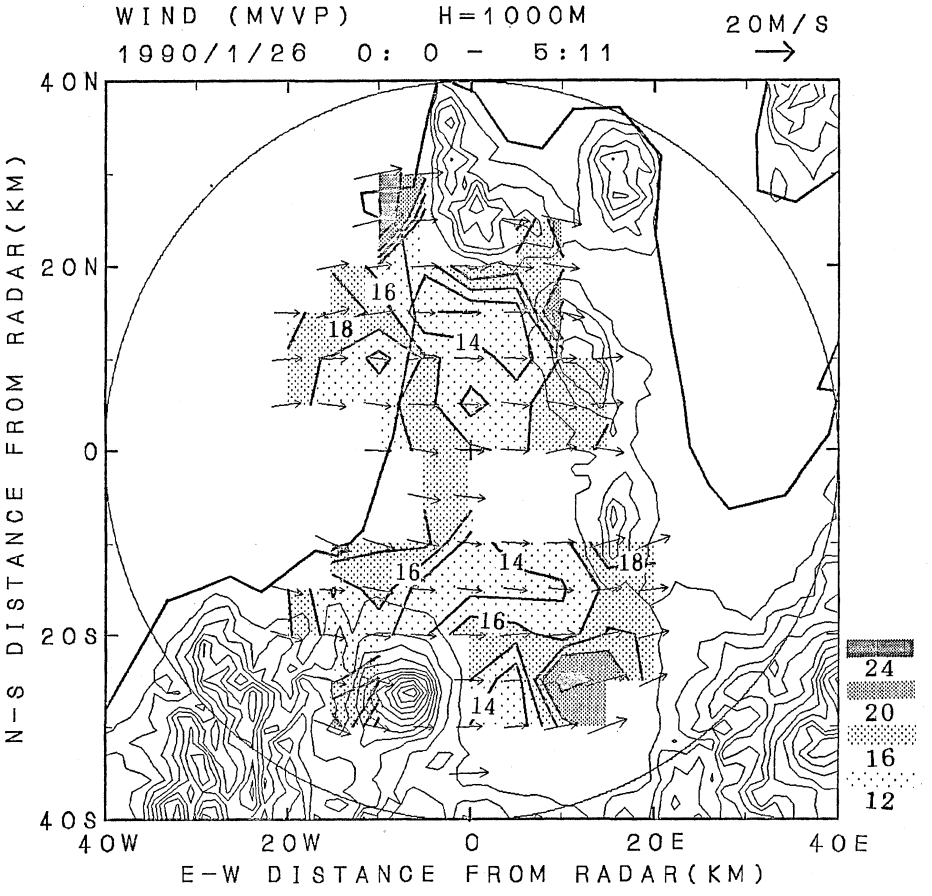

Fig. 14. The same as Fig. 9 except for the period between 0000 and 0511 JST 26 Jan. 1990.

weak-wind zone seemed to maintain this larger-scale updraft.

Over the Tsugaru mountains and in their lee away from the Japan Sea, the displacement between the tops of the echo and of the mixed layer may be large. Not only the lowering of the mixed-layer tops, but the cessation of snow particle production in the uppermost portion of the snow clouds and the gravitational falling of snow particles are possible candidates to form the steep descending of the echo-top around the eastern edge of the weak-wind zone. To evaluate the effect of the gravitational falling, a virtual course of falling snow particles from the crest of the swelled echo-top in the weak-wind zone is shown in Fig. 15(a). Fall velocity of the particles was assumed to be 1.0 m s^{-1}, which is a typical terminal velocity of snow particles, because snow particles seemed to be the major precipitation particles in the uppermost portion of the snow clouds[1]. No vertical wind was assumed, and the horizontal velocity was assumed to be equal to the local evaluated wind speed shown in Fig. 15(b).

The observed eastward inclination of the echo top was somewhat steeper than the virtual course of the snow particles. This displacement between the virtual course and the echo-top inclination suggests the existence of a larger-scale downdraft around the eastern edge of the weak-wind zone, although the gravitational falling speed of snow particles also contributed to the descending of the cloud tops. If a weak convection appeared in the snow clouds, the larger-scale downdraft should be large enough to maintain the observed eastward echo-top inclination against the upward transportation of snow particles by the convective-scale updraft.

As shown in Fig. 16, the maximum echo-top height was larger (smaller) in the upstream of the corridors (peaks) of the Tsugaru mountains. A similar feature was shown in the field of snowfall intensity (Fig. 8). The maximum echo-top height was significantly large along the snowfall zone passing through the central corridor of the Tsugaru mountains. Mechanisms to maintain the snowfall zone will be discussed in Section 5.

4.3 Comparison to a theoretical prediction on flow regime

In this subsection, a possible dynamic link between the weak-wind zone and the Tsugaru mountains is discussed based on a theory of the flow

1 Numerical studies show that not graupel but snow particles are dominant in the uppermost portions of the snow clouds over the Japan islands (*cf.*, Fig. 20 of Murakami *et al.* (1994); Fig. 9 of Saito *et al.* (1996)).

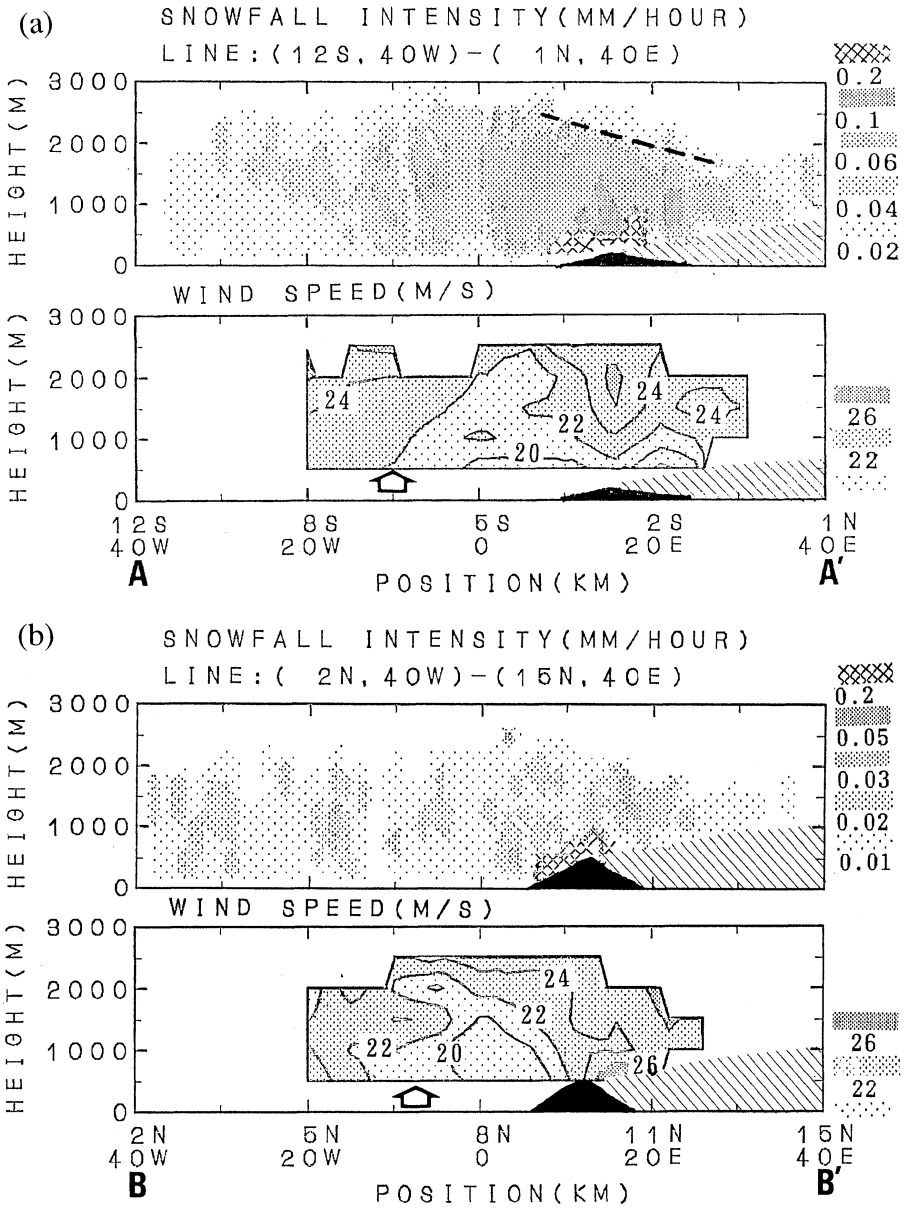

Fig. 15. (a) Vertical cross-section of snowfall intensity (mm hr^{-1}) (upper panel) and wind-speed (m s^{-1}) (lower panel) averaged over the main study period of 1203–1747 JST 25 Jan. 1990, along the A–A' line shown in Figs. 8 and 9. The cross section of the Tsugaru mountains is blacked out. For the upper panel, cross hatch indicates the oozing of ground scattering, while light hatch indicates the regions without radar observation in the shade of mountains. A dashed line indicates a possible course of falling snowflakes. For the lower panel, the wind speed is not shown where reliable wind estimations could not be obtained using the MVVP method. An open arrow indicates the position of the coast line. (b) The same as (a) except along the B–B' line shown in Figs. 8 and 9.

regime of 2–D two-layer flow passing over a ridge proposed by Saito (1992). Since a mixed layer capped by a stable layer was observed during the main study period (Figs. 6 and 12), the airflow over the study area can be approximated as a shallow two-layer flow. The Tsugaru mountains are also approximated as a constant-altitude ridge, although height variation along the ridge is actually large. Saito (1993) showed that a corridor of a ridge strongly modifies the behavior of lee-side hydraulic jump, but weakly influences the upstream blocking by the ridge in his 3–D numerical studies. This allows our 2–D approximation to study the behavior of airflow in the upstream of the Tsugaru mountains.

Saito (1992) classified the flow resume based on the following two environmental parameters: One is Froude Number (Fr) defined by

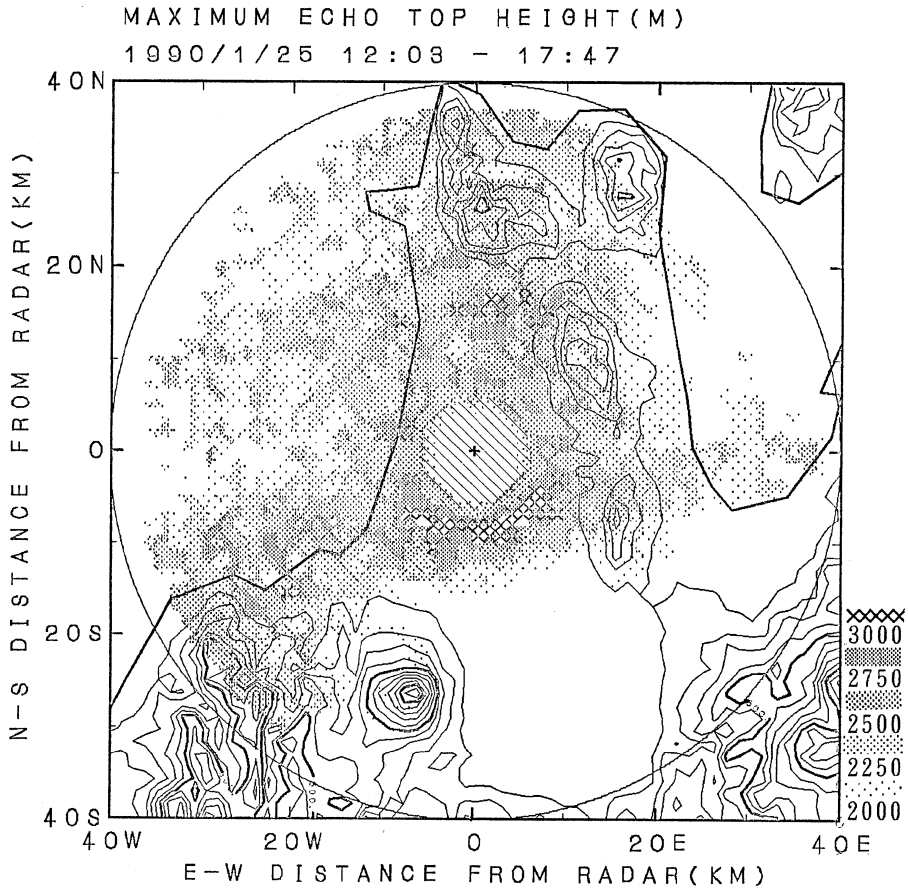

Fig. 16. The maximum height of echo-top (m) during the main study period of 1203–2055 JST 25 Jan. 1990. The area around the site without radar observations is hatched.

$$Fr^2 = U^2 / \left(\frac{\theta' - \theta}{\theta'} \right) \cdot g \cdot h_0, \tag{4}$$

where g is gravity acceleration, U and h_0 are flow speed and depth of the lower layer, and θ' and θ are potential temperature in the upper and lower layers, respectively. The other is a non-dimensional height of the ridge (Mc), defined by

$$\mathrm{Mc} = m_c / h_0, \tag{5}$$

where m_c is the height of the ridge.

These parameters are determined from mean profiles of sonde-observed wind speed and potential temperature at the radar site averaged over the main study period (Fig. 12); $\theta' = 276$ K, $\theta = 264$ K, $U = 20$ m s^{-1}, $h_0 = 3000$ m. m_c is assumed to be 300 m as a mean height of the Tsugaru mountains. These values lead to $Fr = 0.56$ and Mc $= 0.1$. However, the rawinsonde site existed in the weak-wind zone (Fig. 9), where wind speed and depth of the mixed layer were modified from the background over the Japan Sea. Cross sections passing through the vicinity of the site shown in Fig. 15(a) and 15(b) indicate that the wind speed and the top height of the snow clouds were ~ 2 m s^{-1} smaller and ~ 600 m larger, respectively, in the weak-wind zone than over the Japan Sea. If we assume that the tops of the snow clouds approximately followed the depth change of the mixed layer, the depth (h_0) and wind speed (U) of the mixed layer are evaluated to be ~ 2400 m and ~ 22 m s^{-1}, respectively, in the background over the Japan Sea. These values lead to $Fr = 0.69$, and Mc $= 0.13$.

According to Saito (1992), the flow will be subcritical when $Fr = 0.56$, alternatively when $Fr = 0.69$, the flow will be partially blocked accompanied with ascending motion in the upstream of the ridge, and steep descending motion over and in the lee of the ridge accompanied with a hydraulic lee jump. The theoretical prediction of a partial blocking is consistent with the observed weak-wind zone accompanied with ascending motion and the swelled snow clouds in the upstream of the ridge. Observational confirmation of the predicted hydraulic lee jump to the east of the ridge is difficult. This is because the upward extension of the echo top over Mutsu Bay (Fig. 15) cannot be ascribed solely to a lee-jump, but also to orographic ascent by the Natsudomari Peninsula to the east of Mutsu Bay (Fig. 1). On the other hand, stronger surface wind observed downstream of the Tsugaru mountains than in the upstream, is favorable to the existence of a hydraulic lee jump. Surface wind speed averaged for the main study period

was larger at AMeDAS stations in the downstream of the Tsugaru mountains than at the corresponding upstream stations (Fig. 5), *i.e.*, Aomori (9 m s^{-1}) vs. Goshogawara (7 m s^{-1}), and Kanita (6 m s^{-1}) vs. Shiura (4 m s^{-1}).

5. Discussion

5.1 Microphysical process in the snow clouds

As introduced in Section 1, climatological snow depth is large in many places in the lee of the low-altitude ridges in Japan. This suggests intensification of the snow clouds by these ridges. Our results suggest that the upward development of the snow clouds was maintained by an upstream partial blocking by the Tsugaru mountains, however, snowfall intensity did not increase significantly to the east of the crest of the swelled snow clouds (Fig. 8).

Saito *et al.* (1996) suggested that temperature decrease at the tops of the snow clouds due to upward extension of the clouds contributes to increasing the snowfall amount. In their numerical experiment for the snow clouds passing over a ridge including a cloud-physics parameterization, cloud-top temperature of the snow clouds decreased from −19°C to −21°C −23°C accompanied by orographic lifting of the clouds on the windward slope of a ridge. Ice nucleation was activated around the top of the snow clouds by this temperature decrease, and snowfall amount increased as a result of the natural seeding in the snow clouds containing a large amount of supercooled water in their middle and lower portions.

In our case study, top-temperature of the snow clouds was estimated to be ∼ −28°C over the Japan Sea and ∼ −35°C in the weak-wind zone according to the rawinsonde observations. Since the cloud-top temperature in our case was close to a temperature of spontaneous freezing of cloud droplets, the temperature decrease at the cloud tops in the weak-wind zone would not significantly activate the ice nucleation at the uppermost portion of the snow clouds. Moreover the content of supercooled cloud water in the snow clouds would be small, because of low air-temperature in our case contrasting to the experiment of Saito *et al.* (1996). Actually, Murakami *et al.* (1994) showed that ice crystals of high concentration are produced through deposition/sorption nucleation and supercooled cloud water is consumed by the crystals in the snow clouds, in their numerical study of the snow clouds under a low air-temperature condition similar to our case.

For lack of microphysical observations in the snow clouds in our case, we cannot confirm the speculation mentioned above to explain that the snowfall intensity did not increase significantly in spite of the upward development of the snow clouds. Nevertheless, we need to remark on a possibility that the partial blocking induced by the Tsugaru mountains may increase the snowfall amount when air temperature is not as low as in our case, and further studies are expected.

5.2 The snowfall zone in the central portion of the Tsugaru plain

A significant snowfall zone was observed over the Tsugaru plain, accompanied with wind convergence extending from the north of the Shirakami mountains, to Mutsu Bay through the central portion of the Tsugaru plain (Figs. 5, 8, and 10). A similar snowfall zone accompanied with wind convergence has been found in the climatological studies (Fig. 2) (Nibe, 1989; Rikiishi and Hayashi, 1994, 1995) as introduced in Section 1. Although our results on a case cannot be compared directly to the climatology, we show several new 3–D aspects of the snowfall zone observed by the Doppler radar, together with brief comments on irregularities of the snowfall zone in our case in different from climatology.

According to the AMeDAS observations, the surface wind field around the snowfall zone in our case was similar to the climatological one, although the wind direction veered somewhat northward compared to climatology and SW wind over the southern portion of the Tsugaru plain was not observed (Figs. 2 and 5). Nibe (1989) suggested that the climatological SW wind is an outflow from a cold-air pool developed over the southern portion of the Tsugaru plain, where the winter monsoon is interrupted by the Shirakami mountains and Mt. Iwaki and the low-level wind is climatologically weak. Existence of such a cold-air outflow was not suggested in our case, because we found neither the SW wind nor the colder surface air over the southern portion of the Tsugaru plain than over the northern portion (Fig. 5). Further observational studies for cases when the cold SW wind appeared are necessary to examine the roles of the cold-air ourflow for the formation of the snowfall zone.

The WNW wind over the northern part of the Tsugaru plain was detectable in the surface wind field observed by AMeDAS, but not in the upper-level wind fields derived by the MVVP method (Figs. 5 and 10). This indicates that the WNW wind was confined to the surface.

When examining possible mechanisms which intensified the snowfall zone, the following two characteristics must be considered in addition to the wind convergence remarked in the climatological studies: 1) Development of the zone began on the north of the Shirakami mountains and Mt. Iwaki before entering the Tsugaru plain; 2) The zone passed through a corridor of the Tsugaru mountains.

The development of the snowfall zone to the north of the Shirakami mountains and Mt. Iwaki is also supported by locally higher maximum echo-top height (Fig. 16), and strong wind convergence (Fig. 10). Since these mountains exceed the Tsug-

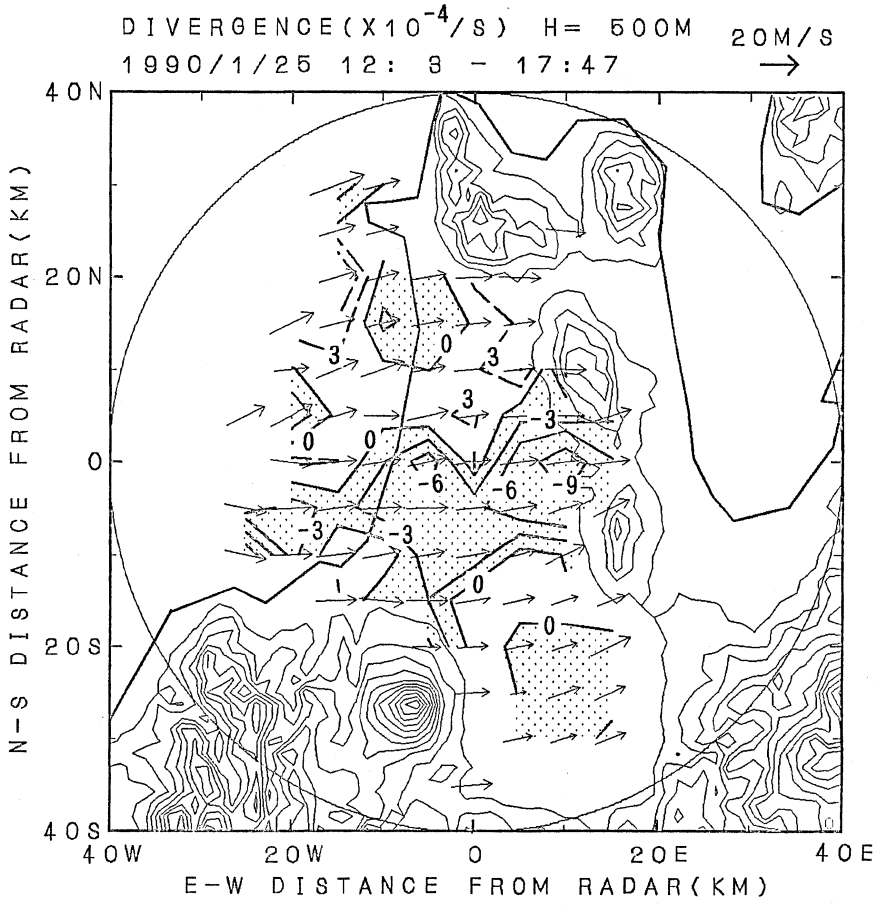

Fig. 17. Same as in Fig. 10 except at 500 m AGL.

aru mountains in elevation and horizontal extension, the airflow may prefer to go around than to pass over them. The convergence zone may be sustained between the orographically-veered wind going around these high-altitude mountains, and the large-scale wind prevailed over the Japan Sea. To make a conclusive discussion, however, we need to examine the wind field over a larger area including the upstream of the Shirakami mountains.

As shown in Fig. 1, the Tsugaru mountains has three corridors around 200 m ASL and three peaks around 500 to 700 m ASL on the ridge. The snowfall zone extended through the central corridor at a position of ($\sim$ 0, $\sim$ 15E) (Fig. 8). Figure 17 shows the mean field of wind and wind divergence at 500 m AGL averaged over the main study period. Convergent flow toward the central corridor was significant at the entrance of the central corridor, where wind convergence was much stronger at 500 m AGL than at 1000 m AGL (Fig. 10). Since the peaks of the Tsugaru mountains neighboring the central corridor are around 500 m high ASL (Fig. 1), the stronger wind convergence at 500 m AGL appeared to be orographically induced. Saito (1993) showed that wind-speed of a flow passing over a ridge increases significantly in a corridor of the ridge in his numerical study.

This low-level wind convergence at the entrance of the corridor may intensify the snowfall around, and in the downstream of the corridor. Although snowfall intensity near the ground surface on the corridor was not observable due to contamination of ground scattering, rather strong snowfall exceeding 0.1 mm hr^{-1} was found below 1000 m AGL above and in the lee of the corridor (Fig. 15(a)), which may be ascribed to the orographic intensification of snowfall by the corridor. Fujiyoshi *et al.* (1996) found that a seeder-feeder mechanism intensified the snowfall over Nobi Plain of Japan ($\sim$ 35°N, $\sim$ 137°E) between orographically induced low-level clouds and upper-level clouds advected from the Japan Sea. A seeder-feeder process between low-level clouds intensified by the convergence at the entrance of the corridor, and the snow clouds advected from the Japan Sea may be a possible mechanism to maintaining the intensified snowfall around the corridor. According to surface meteological observations performed at a position of ($\sim$ 5S, $\sim$ 5E) in the Tsugaru Plain (Sato *et al.* 1994), daily-averaged surface temperature, relative humidity, and pressure of 25 Jan. 1990 were −8.6°C, 91.2 %, and 1017.1 hPa. These values lead to a lifting condensation level (LCL) of no

more than $\sim$ 200 m. If we suppose that this LCL was a typical value over the Tsugatu Plain during the main study period, low-level clouds were possibly developed around the corridor by an orographic updraft, because both the corridor ($\sim$ 200 m ASL) and its neighboring peaks of the Tsugaru mountains ($\sim$ 500 m ASL) are higher than the LCL. However, we cannot make a conclusive discussion about the seeder-feeder process, because there were no observational information about the existence and the microphysical structure of the low-level clouds around the corridor.

Another interesting feature is that snowfall activity in the upstream of the Tsugaru mountains was intensified (suppressed) in the upstream region of each corridor (each peak) of the ridge (Fig. 8). This variance was detectable at distances greater than 60 km upstream of the ridge. Based on his 3–D numerical experiments, Saito (1993) showed that the influence of height variation along a ridge to airflow passing over the ridge is much stronger in the downstream than in the upstream. His results, however, indicate that low-level wind speed is rather larger (smaller) in the upstream of corridors (peaks) of a ridge, and this wind-speed variation extends to several ten kilometers upstream of the ridge (Fig. 8 of Saito 1993). Unfortunately, resolution and accuracy of the wind evaluation by the MVVP method in our case was not enough to confirm the upstream wind-speed variation accompanied with the height variation along the Tsugaru mountains. Dual Doppler radar observations are necessary to examine the influence of the height variation along the ridge.

6. Summary and remark

The influence on behavior of the snow clouds and airflow by a complex terrain in the Tsugaru district has been investigated based on observation data using a single Doppler radar and launched rawinsondes. Since no meso-scale disturbances were identified in the vicinity of the study area, we can isolate the orographic effect on the snow clouds and airflow. The main results of this study are summarized as follows:

1) A weak-wind zone appeared about 15 km upstream of the Tsugaru mountains with height of 200 m to 700 m ASL, accompanied by a strong-wind zone above and in the lee of the mountains. Low-level wind convergence and divergence were observed along the western and eastern edges of the weak-wind zone, respectively, consistent with the wind-speed variation across the zone;

2) The snow clouds extended upward around the western edge of the weak-wind zone and the maximum cloud-top height occurred in the weak-wind zone. While above the Tsugaru mountains and in their lee, tops of the snow clouds descended steeply toward the east, and then ascended again over Mutsu Bay;

3) A theory of 2–D two-layer flow passing over a ridge predicted a flow regime where the flow is partially blocked by the ridge under sonde-observed environmental parameters. The observed flow pattern passing over the Tsugaru mountains was consistent with this prediction, and the observed weak-wind zone was maintained by a partial blocking by the Tsugaru mountains. The descending flow above and in the lee of the Tsugaru mountains and the hydraulic lee jump were not confirmed due to observational difficulties, however, the echo-top-height variation of the snow clouds and surface wind-speed variation around the Tsugaru mountains was consistent with a hydraulic lee jump;

4) Height variation along the Tsugaru mountains also affected the upstream snowfall activity. Snowfall intensity and echo-top height was larger (smaller) in the upstream of the corridors (peaks) of the Tsugaru mountains. This variation of the snowfall activity was detectable at ranges greater than 60 km upstream of the ridge;

5) Among the intensified snowfall areas in the upstream of the corridors, a snowfall zone passing through the central corridor of the Tsugaru mountains was especially significant and extended from on the north of the Shirakami mountains and Mt. Iwaki, high-altitude mountains, to Mutsu Bay accompanied with strong low-level wind convergence. We discussed possible contributions of these high-altitude mountains and of a corridor of the Tsugaru mountains to maintaining this snowfall zone.

Finally, we remark that the behavior of the snow clouds in the upstream of low-altitude ridges may strongly affect the snowfall intensity in the lee, because the snow clouds may easily pass over low-altitude ridges toward the lee side as observed in our case study (Figs. 15(a) and 15(c)). Further studies on the general behavior of the snow clouds in the upstream of low-altitude ridges are needed to clarify the influence of ridges to snowfall activity, both in the upstream and downstream regions of the ridges.

Acknowledgments

The authors thank Dr. H. Nakamura, an ex-Head of Nagaoka Institute of Snow and Ice Studies, NIED, who provided the data of low-level rawinsonde observations at the radar site. Thanks are extended to Mr. H. Nibe, an ex-Head of Miyako observatory of

JMA, for use of his figures on climatological snowfall and surface wind fields in Aomori Prefecture, and to Dr. A. Sato, the Head of Shinjo Branch of Snow and Ice Studies, NIED, for providing surface meteorological observation data. We also thank anonymous referees for variable constructive comments during the review. Many suggestions by Dr. S.L. Hopkins were useful to improve the English expression of the original manuscript. The NCAR Graphics was utilized to draw many figures in this paper.

References

Asai, T., and K. Nakamura, 1978: A numerical experiment of air mass transformation processes over warmer sea. Part I: Development of a convectively mixed layer. *J. Meteor. Soc. Japan*, **56**, 424–434.

Fujiyoshi, Y., 1992: Snowfall and topography. *Meteorology of the water cycle, Lectures on Meteorology 3* (T. Asai and T. Matsuno ed.), University of Tokyo Press, 41–58 (in Japanese).

Fujiyoshi, Y., T. Endoh, T. Yamada, K. Tsuboki, Y. Tachibana and G. Wakahama, 1990: Determination of a Z-R relationship for snowfall using a radar and high sensitivity snow gauges. *J. Appl. Meteor.*, **29**, 147–152.

Fujiyoshi, Y., T. Fujita, T. Takeda, T. Kojiri, K. Takara and S. Ikeda, 1996: The effect of complex terrain on the leeside distribution of snowfall -In the case of Nobi Plain- (in Japanese). *Tenki*, **43**, 391–408.

Higashiura, M., 1990: An introduction of the studies on clarification of drifting snow occurrence performed by National Research Institute for Earth Science and Disaster Prevention (in Japanese). *Seppyo*, **52**, 224–225.

Kanada, S., B. Geng, N. Yoshimoto, Y. Fujiyoshi and T. Takeda, 1999: Doppler radar observation on the orographic modificatrion of a precipitating convective cloud in its landing. *J. Meteor. Soc. Japan*, **77**, 135–154.

Kodama, Y.-M., T. Nakayama and N. Osaki, 1995: Precipitation variations over the north-eastern part of Japan on a scale of one or several hundred kilometers during winter monsoon periods (in Japanese). *Tenki*, **42**, 85–96.

Kondo, J., 1976: Heat balance of the East China sea during the Air Mass Transformation Experiment. *J. Meteor. Soc. Japan*, **54**, 382–398.

Koscielny, A.J., R.J. Doviak and R. Rabin, 1982: Statistical considerations in the estimation of divergence from single-Doppler radar and application to prestorm boundary-layer observations. *J. Appl. Meteor.*, **21**, 197–210.

Maki, M., T. Yagi and S. Nakai, 1989: The doppler radar of NRCDP and observations of meso-scale weather systems. *Report of the National Research Center of Disaster Prevention*, **44**, 61–79.

Maki, M., S. Nakai, T. Yagi and H. Nakamura, 1992: Doppler radar observations of snow storms: L-mode case (in Japanese). *Tenki*, **39**, 551–563.

Murakami, M., T.L. Clark and W.D. Hall, 1994: Numerical simulations of convective snow clouds over the Sea of Japan; two-dimensional simulations of mixed layer development and convective snow cloud formation. *J. Meteor. Soc. Japan*, **72**, 43–62.

Nakai, S., M. Maki and T. Yagi, 1990: Doppler radar observation of orographic modification of snow clouds - A case of enhanced snowfall - (in Japanese with an English abstract). *Report of the National Research Center for Disaster Prevention*, **45**, 1–16.

Nakai, S. and T. Endoh, 1995: Observation of snowfall and airflow over a low mountain barrier. *J. Meteor. Soc. Japan*, **73**, 183–199.

Nibe, H., 1989: Weathers in Aomori Prefecture. Hoppo Shinsha. 282 pp.

Pierrehumbert, R.T. and B. Wyman, 1985: Upstream effects of mesoscale mountains. *J. Atmos. Sci.*, **42**, 977–1003.

Rikiishi, K. and T. Hayashi, 1994: On the snowfall over the Tsugaru plain due to orographic convergent winds (in Japanese). *Tohoku-no Yuki to Seikatsu* (Published by the Tohoku branch of the Japanese Society of Snow and Ice), **9**, 30–32.

Rikiishi, K. and T. Hayashi, 1995: On the snowfall at Aomori City due to orographic convergent winds (in Japanese with an English abstract). *Seppyo*, **57**, 221–228.

Saito, K., 1992: Shallow water flow having a lee hydraulic jump over a mountain range in a channel of variable width. *J. Meteor. Soc. Japan*, **70**, 775–782.

Saito, K., 1993: A numerical study of the local downslope wind "Yamaji-kaze" in Japan Part 2: Non-linear aspect of the 3-D flow over a mountain range with a col. *J. Meteor. Soc. Japan*, **71**, 247–271.

Saito, K., L. Thanh and T. Takeda, 1994: Airflow over the Kii peninsula and its relation to the orographic enhancement of rainfall. *Pep. Meteor. Greophys.*, **45**, 65–90.

Saito, K., M. Murakami, T. Matsuo and H. Mizuno, 1996: Sensitivity experiment on the orographic snowfall over the mountainous region of northern Japan. *J. Meteor. Soc. Japan*, **74**, 797–813.

Sasaki, Y., M. Maki and K. Iwanami, 1998: Error analysis of the MVVP method applied to nonlinear wind field (in Japanese with an English abstract). *Report of the National Research Institute for Earth Science and Disaster Prevention*, **58**, 121–136.

Sato, A., M. Higashiura and T. Sato, 1994: Meteorological data of winter at the Tsugaru plain, Aomori prefecture (Decemver 1986–March 1993) (in Japanese with an English abstract). *Technical Note of the National Research Institute for Earth Science and Disaster Prevention*, **161**, 1–40.

Tatehira, R. and O. Suzuki, 1994: Accuracy in estimation of wind velocity from a single Doppler radar (in Japanese). *Tenki*, **41**, 761–764.

Tatehira, R., Y. Murata and O. Suzuki, 1998: Accuracy in estimating horizontal divergence from a single Doppler radar (in Japanese). *Tenki*, **45**, 249–257.

低い山脈の風上側に形成された弱風域と上方に発達した降雪雲
—津軽地方における1台のドップラーレーダーによる観測—

児玉安正
（弘前大学理工学部）
真木雅之[1]
（防災科学技術研究所）
安藤真一[2]・大槻政哉[2]・稲葉　修[3]・猪上　淳[4]・越前直哉[5]
（弘前大学理学部）
中井専人・八木鶴平
（防災科学技術研究所）

日本海上で冬季季節風が吹くと、多くの背の低い対流性雪雲が大気混合層内に生じ、日本列島に多量の降雪をもたらす。津軽地方の複雑な地形の影響を受けた雪雲と気流の振舞いを1台のドップラーレーダーによる観測で調べた。標高が200～700 mの背の低い山脈である津軽山地の風上側～15 kmの領域に山地に平行に伸びる帯状の弱風域がみられ、そこで雪雲の雲頂が上方に盛り上がっていた。一方、津軽山地の上空とその風下では風速が増加すると共に雪雲の雲頂が急激に低下していた。山越えする二層流体の2次元の理論によると、ゾンデ観測から得られた環境パラメータ下では、山脈の風上の部分ブロッキング、山頂から風下での下降流と風下ジャンプを伴う流れが予想された。観測的な限界から十分な確認ができなかった下降流と風下ジャンプを除くと、観測結果はこの理論的予想と矛盾しない。弱風域の入り口での下層収束は雪雲を上方へ発達させていた。しかし上方への発達にともなう降雪強度の増加は確認できなかった。標高が1000 mを越える白神山地や岩木山の北方から津軽平野の中部を通って陸奥湾まで、西南西－東北東の方向に伸びる顕著な帯状の強降雪域が観測された。この帯状降雪域を維持するメカニズムとして、白神山地と岩木山、及び津軽山地の鞍部の地形的影響を検討した。

1　現所属：気象研究センター（オーストラリア）
2　現所属：日本気象協会北海道本部
3　現所属：気象庁仙台管区気象台
4　現所属：北海道大学低温科学研究所
5　現所属：北海道地図株式会社